

# Synthesis and Studies of Ferroelectric Metal-Organic Cages and Frameworks

*A Thesis*

*Submitted in partial fulfilment of the requirements for the*

*BS-MS Dual Degree Programme*

*by*

**Rani Gourkhede**

**(20151154)**

*Under the guidance of*

**Prof. R. Boomi Shankar**



**Indian Institute of Science Education and Research Pune**

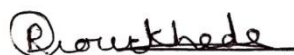
**Dr. HomiBhabha Road,**

**Pashan, Pune 411008, INDIA.**

**April, 2020**

# Certificate

This is to certify that this dissertation entitled “**Synthesis and Studies of Ferroelectric Metal-Organic Cages and Frameworks**” towards the partial fulfilment of the BS-MS dual degree programme at the Indian Institute of Science Education and Research, Pune represents study carried out by **Rani Gourkhede** at Indian Institute of Science Education and Research under the supervision of **Prof. R. Boomi Shankar**, Professor, Department of Chemistry, during the academic year 2019-2020.



Rani Gourkhede

20151154



Prof. R. Boomi Shankar

Supervisor

Committee:

Supervisor :**Prof. R. Boomi Shankar**

Professor, Department of Chemistry

IISER Pune

Email: [boomi@iiserpune.ac.in](mailto:boomi@iiserpune.ac.in)

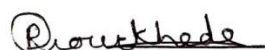
TAC :**Dr. Shabana Khan**

Assistant Professor, Department of

Chemistry IISER Pune

# Declaration

I hereby declare that the matter embodied in the report entitled “**Synthesis and Studies of Ferroelectric Metal-Organic Cages and Frameworks**” are the results of the work carried out by me at the Department of Chemistry, Indian Institute of Science Education and Research, Pune, under the supervision of **Prof. R. Boomi Shankar** and the same has not been submitted elsewhere for any other degree.



**Rani Gourkhede**

20151154



**Prof. R. Boomishankar**

Supervisor

Professor, Department of Chemistry  
IISER Pune

Email: [boomi@iiserpune.ac.in](mailto:boomi@iiserpune.ac.in)

**This thesis is dedicated to**  
**My Mother....**

# Acknowledgments

---

At very first, I would like to express my sincere gratitude and respect for my thesis supervisor **Prof. R. Boomi Shankar** for his continuous support during my research period and for giving me an opportunity to work in his lab from my fourth year of BS-MS onwards. His valuable guidance, immense knowledge and regular discussions helped me to overcome all the problems I faced and finish my project smoothly. His strong motivation has always directed me well in research and life as well.

I am also thankful to my TAC member Dr. Shabana Khan for her regular support and vital suggestions in my research work. It is my privilege to be a part of the Indian Institute of Science Education and Research, Pune and I would like to acknowledge all the faculty members for their brilliant teaching which helped me to keep up my interest in science. I am grateful to the Department of Science and Technology (DST), for the financial support by providing me INSPIRE fellowship throughout my years in IISER Pune.

A big thank to my lab members Ms. Neetu Prajesh, Ms. Swati Deswal, Mr. T Vijaykanth, Mr. Rishabh Gupta, Mr. Rajasekar, Ms. Meghamala Sarkar, Ms. Supriya Sahoo and Mr. Rishu Panday for their great support, lively lab environment, for listening to my doubts to guiding me from very start.

I would like to express my deep gratitude towards my parents for their unconditional love and strong believe in me. I am grateful to my both sisters for always having my back and their constant support and care. I am forever thankful to my family for giving me the best suggestions and experiences which made me who I am. I owe everything to them.

This journey would not have been complete without my good friends Ms. Akansha Gupta, Mr. Kunjan Patel, Mr. Hrthik Gudapati, Ms. Arati Jadhav, Ms. Nupur Sontakkey, Mr. Mahendra Patel, Ms. Shana Shirin, Ms. Heena Suthar, Ms. Kiran Roy . I am immensely thankful for their support, care, and beautiful friendship. Lastly, I am thankful to all those who ever helped me in any way possible.

Rani Gourkhede

# Table of Contents

---

<b>Chapter 1: Introduction</b> .....	1-8
1.1 Introduction to Ferroelectric Metal-Organic Self Assemblies .....	1
1.2 Dielectric Materials.....	1
1.2.1 Polarization in Dielectric Materials.....	1
1.2.1.1 Electronic Polarization .....	2
1.2.1.2 Ionic/Atomic Polarization.....	2
1.2.1.3 Dipolar/Orientational Polarization .....	2
1.2.1.4 Space Charge Polarization.....	2
1.2.2 Frequency and Temperature effect on Dielectric Polarization.....	3
1.2.3 Dielectric Constant .....	3
1.2.4 Applications of Dielectric Material .....	3
1.3 Classification of Dielectrics .....	3
1.4 Piezoelectric Materials.....	4
1.5 Pyroelectric Materials .....	4
1.6 Ferroelectric Materials .....	5
1.7 History of Ferroelectric Materials .....	6
1.8 Application of Ferroelectric Materials.....	6
1.9 Metal-Organic Ferroelectric Materials .....	7-8
<b>Chapter 2: Materials and Methods</b> .....	9-10
2.1 General Remark.....	9
2.2 Synthesis .....	9
2.2.1 Synthesis of ligand .....	9
2.2.2 Synthesis of compound.....	9
2.3 Crystallography .....	10
2.4 Ferroelectric and Dielectric measurements.....	10

<b>Chapter 3: Results and Discussion .....</b>	<b>11-18</b>
3.1 Syntheses .....	11
3.2 Crystal Structures .....	12
3.3 Ferroelectric and Dielectric Studies .....	13-16
3.3.1 Ferroelectric Results .....	13-14
3.3.2 Dielectric studies .....	14-16
3.4 Solvent dependent studies of Compound 1 .....	17-18
3.4.1 TGA .....	17
3.4.2 FT-IR .....	18
3.4.3 PXRD .....	18
<b>Conclusion .....</b>	<b>19</b>
<b>References .....</b>	<b>20-21</b>

# List of Figures

Figure no.	Title	Page no.
1.1	Polarization in dielectric material in external applied electric field.	1
1.2	Classification of dielectric materials based on crystal classes.	3
1.3	Typical ferroelectric hysteresis loop.	6
1.4	Paraelectric-ferroelectric phase transition.	6
1.5	Application of ferroelectrics.	7
3.1	View of compound <b>1</b> octahedral cage (a) along 3- fold axis (b) along 4-fold axis.	13
3.2	Ferroelectric hysteresis loop for compound <b>1</b> at frequency 0.01 Hz.	14
3.3	Frequency dependent P-E loop.	14
3.4	Plots of the real part of the dielectric permittivity (a) vs. frequency, (b)vs. temperature	15
3.5	Plots of the dielectric loss (a) as a function of temperature, (b) as a function of frequency.	16
3.6	(a) TGA and DTA plots of compound <b>1</b> , (b) TGA plots of <b>1</b> , <b>1</b> <sub>desolvated</sub> , and <b>1</b> <sub>resolvated</sub> .	17
3.7	IR spectra for <b>1</b> , <b>1</b> <sub>desolvated</sub> , and <b>1</b> <sub>resolvated</sub> .	18
3.8	PXRD pattern of <b>1</b> , <b>1</b> <sub>desolvated</sub> , and <b>1</b> <sub>resolvated</sub> .	19



## List of Tables

<b>Table no.</b>	<b>Title</b>	<b>Page no.</b>
<b>1.1</b>	Occurring frequency of different ways of polarization.	<b>2</b>
<b>2.1</b>	Details of crystallographic data collection	<b>10</b>

## List of Schemes

<b>Scheme no.</b>	<b>Title</b>	<b>Page no.</b>
<b>3.1</b>	Synthesis of ligand TPPA.	<b>13</b>
<b>3.2</b>	Schematic of Compound <b>1</b> formation.	<b>14</b>

# Abbreviations

TPPA	tris(3-pyridinyl) phosphoric triamide)
SCXRD	Single Crystal X-ray Diffraction
$P_r$	Remnant Polarization
$P_s$	Saturation Polarization
$E_c$	Coercive field
AC	Alternating Current
$T_c$	Curie Temperature
Hz	Hertz
mmol	millimole
mg	milligram
MeOH	Methanol
P-E	Polarization vs. Electric Field
MALDI-TOF	Matrix-Assisted Laser Desorption/Ionization – Time of Flight
TGA	Thermogravimetric Analysis
ATR	Attenuated total reflectance
NMR	Nuclear Magnetic Resonance
FT-IR	Fourier Transform Infrared Spectroscopy
PXRD	Powder X-ray Diffraction
DTA	Differential Thermal Analysis

# Abstract

---

Ferroelectric properties derived from the metal-organic assemblies have attracted significant attention as an alternate choice of the conventional inorganic ceramics due to their fascinating structural architectures, simple protocol of synthesis and no potential toxic elements. Here, a new discrete octahedral metal-organic cage  $[\text{Cu}_6(\text{H}_2\text{O})_{12}(\text{TPPA})_8] \cdot (\text{NO}_3)_{12} \cdot (\text{H}_2\text{O})_{24}$  has been synthesized using a flexible tripodal ligand TPPA (TPPA=tris(3-pyridinyl) phosphoric triamide).

SCXRD analysis reveals that the cage is crystallized in non-centrosymmetric polar space group ( $I4$ ) which is suitable to show ferroelectric behaviour. Ferroelectric measurements were performed on the powder pressed pellet at room temperature on the Sawyer-Tower circuit. The well resolved rectangular P-E hysteresis loop was obtained exhibiting high remnant polarization ( $P_r$ ) of  $39.23 \mu\text{Ccm}^{-2}$  at 0.1 Hz. The switching rate strongly affects the dynamics of the domain walls which is clearly reflected in the frequency dependent studies of P-E loop which shows a significant decrease in the  $P_r$  values when increasing the AC frequency. The ferroelectric response is due to the ordering of disordered nitrate ions and solvate molecule which is present between the pockets of the cages. Solvent dependent studies confirm the reversible nature of desolvation and resolvation in this cage.

# Chapter 1

## Introduction

### 1.1 Introduction to Ferroelectric Metal-Organic Self Assemblies

Ferroelectric materials are a special type of dielectrics with spontaneous electric polarization which can be reversed by the application of an external electric field.<sup>1</sup> Over the past decades, substantial studies have been made on materials with ferroelectric properties from which metal-organic self assemblies have gained remarkable attention due to their simple synthesis protocols, fascinating structural architectures, manageability for low temperature, low cost, non-toxicity, and their potential for numerous applications.<sup>2,3</sup> These assemblies entails various interactions such as hydrogen-bonding, ionic, coordination etc. between organic ligands and metal ions to form discrete to higher dimensional structures.<sup>4</sup>

### 1.2 Dielectric Materials

Dielectric materials are electrical insulators, which can be polarized in the presence of an external electric field. Even if they are non-conductive materials, because of an applied electric field there is marginally shift in charges within dielectrics which leads to creating electric dipoles in system.<sup>5</sup> The density of these induced electric dipole moments called dielectric polarization.

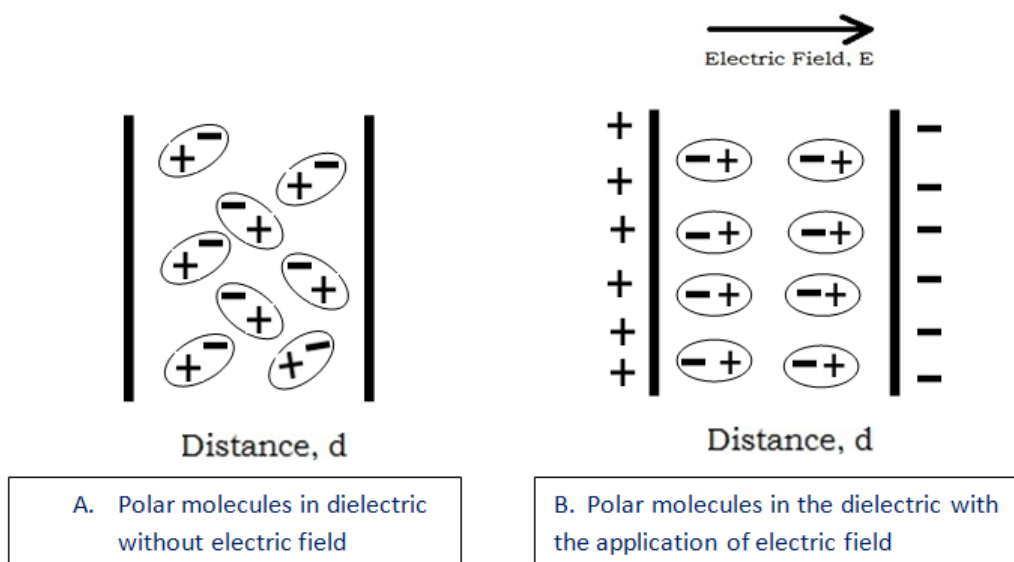


**Figure 1.1:** Polarization in dielectric material in external applied electric field.

## **1.2.1 Polarization in Dielectric Materials**

In the absence of electric field an atom is neutral by balancing the positively and negatively charged particles, but when we apply electric field charges are imbalanced by the following polarization mechanisms.<sup>6,12</sup>

### **1.2.1.1 Electronic Polarization**

In neutral atom nucleus is surrounded by the electronic cloud which would move from original position towards positive electrode on the application of an external electric field. Thus this is an induced polarization effect. The magnitude of electronic polarization is smaller than other polarization pathways.<sup>5,7</sup>

### **1.2.1.2 Ionic/Atomic Polarization**

It is related to the displacement of ions, it occurs in the ionic compound when the bond between ions get stretched in the presence of electric field and changes the dipole moment of the molecule. Since the ionic bond is strong there is no displacement of high magnitude, but it is higher than electronic polarization.<sup>5,7</sup>

### **1.2.1.3 Dipolar/Orientational Polarization**

It is present in dipolar materials with permanent dipole moments. Initially all dipoles are present in a random direction and hence there is no net dipole moment in system. When we apply electric field molecule having a permanent dipole moment align themselves in the direction of electric field and gives net dipole moment to system.<sup>5,7</sup>

### **1.2.1.4 Space Charge Polarization**

It is produced by the movement or migration of charge carriers by some distance through dielectric material (via hopping, diffusion etc.) in the existence of an electric field. This charge carriers movement can be terminated by an interface which leads to space charge formation.<sup>5,7</sup>

## **1.2.2 Frequency and Temperature effect on Dielectric Polarization**

Dielectric polarization which includes movements of ions or electrons are highly dependent on the frequency of the applied electric field and the one with higher mass will take more time to displace than a lighter one.

**Table 1.1:** Occurring frequency of different ways of polarization.

<b>Polarization type</b>	<b>Occurring frequency</b>
Electronic polarization	$\sim 10^{13}-10^{15}$ Hz
Ionic polarization	$\sim 10^9-10^{13}$ Hz
Dipolar polarization	Below $10^9$ Hz
Space charge polarization	Below 10 Hz

Dielectric polarization exhibits dependence on temperature. In ionic systems increase in temperature increases the ion mobility and charge carriers which enhance the polarization. While in the case of dipolar polarization as the temperature increases the polarization effect is decreased because of increase in thermal agitation.<sup>8</sup>

### 1.2.3 Dielectric Constant

Dielectric constant tells about the ability of dielectric material to store electric energy when an electric field is applied. It is also known as relative permittivity ( $\epsilon_r$ ).

$$\epsilon_r = \epsilon / \epsilon_0 \dots \text{Eq 1.1}$$

where  $\epsilon$  is the absolute permittivity of material and  $\epsilon_0$  is the permittivity of vacuum

It is also calculated as a ratio of the capacitance of parallel plate electrodes.

$$\epsilon_r = C_m / C_0 \dots \text{Eq 1.2}$$

where  $C_0$  is capacitance when there is vacuum between two plate electrodes and  $C_m$  is when a dielectric material is filled between two plates.<sup>5,8,10</sup>

### 1.2.4 Applications of Dielectric Materials

Dielectric materials with a high dielectric constant are used for charge storage in capacitors, materials with a low dielectric constant are utilized in microelectronic circuits as electrical insulators. Dielectrics are also used in transducers, heating devices, resonators, power transformers and other high technique applications.<sup>5,8,10</sup>

### 1.3 Classification of Dielectrics

Linear dielectrics show linear nature between polarization and applied electric field. On the removal of the electric field, this dielectric material get depolarized.<sup>14</sup>By the mechanism of polarization this class is further divided into

- Non-polar materials
- Polar materials

There are some dielectric materials that show high dielectric constant which indicate non-linearity between polarization and applied electric field are called as non-linear dielectrics. They may have non zero polarization when no electric field is applied. This special class of dielectrics exhibit unusual properties.<sup>8,9</sup>

Based on the crystal classes, the non-linear dielectrics shows important physical properties, which include ferroelectricity, pyroelectricity and piezoelectricity. In total there are 32 crystal classes, from which 11 are centrosymmetric and the remaining 21 are non-centrosymmetric crystal classes. From all non-centrosymmetric crystal classes 20 classes show piezoelectricity and out of 20 there are 10 polar crystal classes which exhibit ferroelectricity and pyroelectricity.<sup>8,9,11</sup>

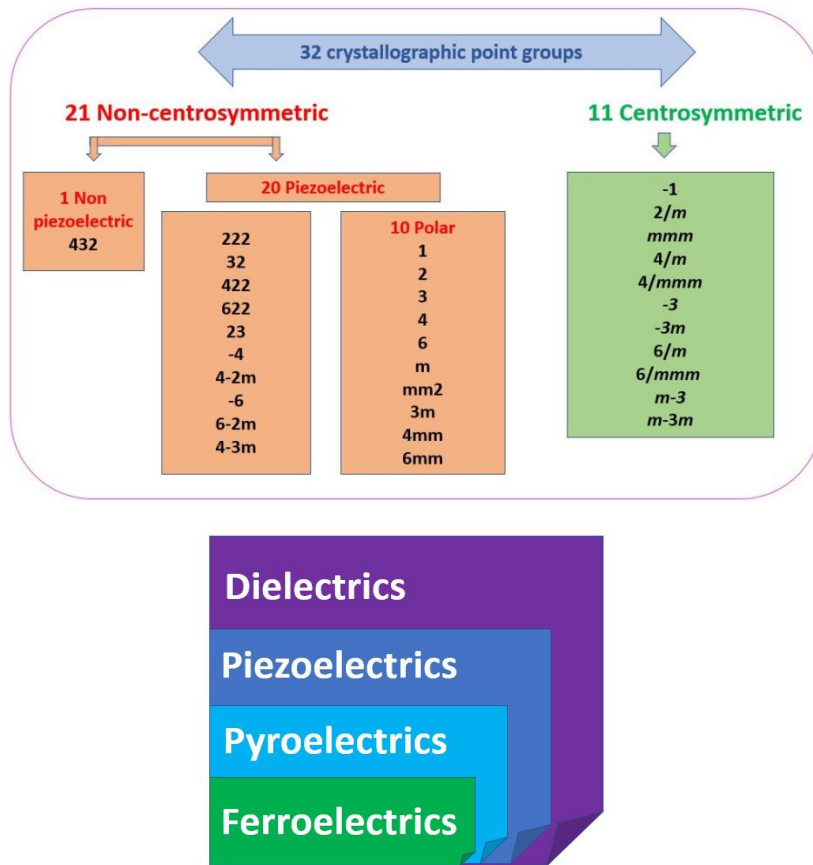


**Figure 1.2:** Classification of dielectric materials based on crystal classes.

## 1.4 Piezoelectric Materials

In 1880 Curie brothers, Pierre and Jacques, first demonstrated the direct piezoelectric effect. Piezoelectric materials are a special class of non-linear dielectrics which on application of mechanical strain accumulate electric charge in response. Some naturally occurring piezoelectric crystals are quartz, sucrose, Rochelle salt, topaz, tourmaline etc. Piezoelectric materials are used in various applications such as medical devices, sonar devices, actuators, sensors, telecommunications etc.<sup>5,8</sup>

## 1.5 Pyroelectric Materials

Pyroelectric materials are those materials which generate electric potential when there is thermal gradient produced around them. This effect was first discovered by Theophrastus in 314 BC.

As they are responsive to changes in temperature pyroelectric materials are mainly used in infrared detectors, intruder alarms, energy harvesting etc.<sup>5,8</sup>

## 1.6 Ferroelectric Materials

Ferroelectric materials are a special type of dielectric materials with spontaneous electric polarization which can be reversed by the application of an external electric field. The compound should be crystalline in nature and must adopt polar non-centrosymmetric point group to show ferroelectricity.<sup>15</sup>

Ferroelectric materials show a hysteresis loop which is a plot between their polarization (P) vs applied electric field (E). When we increase the strength of electric field polarization of ferroelectric material also increases and at the higher value of the electric field it reaches to a saturation polarization ( $P_s$ ). After the removal of applied electric field there is still some polarization at zero field called as remnant polarization ( $P_r$ ) and the field required to reverse the direction of polarization is termed as a coercive field ( $E_c$ ) and when we increase electric field beyond  $E_c$  we get polarization in a reverse direction.<sup>5,8,9</sup>

Temperature plays a vital role in the observation of ferroelectricity in a material. At high temperatures, most of the crystals drop their polar alignments of dipoles and become non polar whereas on cooling crystal again gain polar alignments of dipoles. A temperature below/at which crystals show ferroelectricity called as Curie temperature ( $T_c$ ).

The paraelectric-ferroelectric phase transition are of two types : a) Displacive : In this displacement of ions occurs below  $T_c$  b) Order-disorder : Dipolar ions reassemble to achieve polar order below  $T_c$ .<sup>8,9,16</sup>



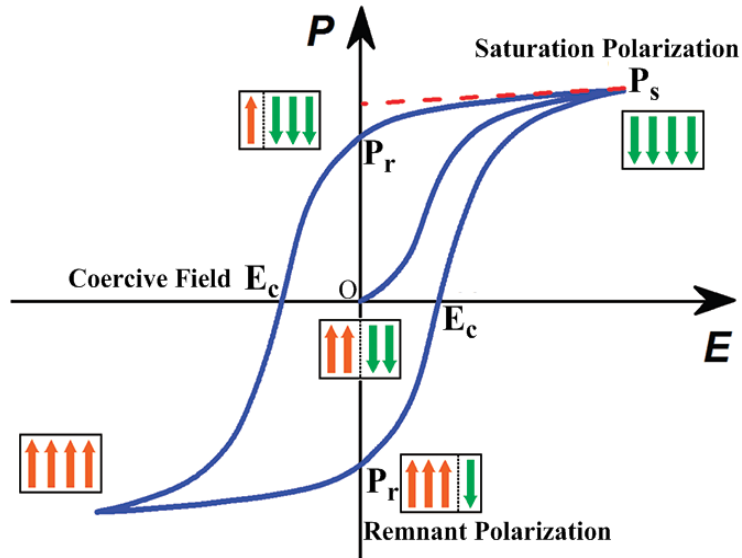


Figure 1.3: Typical ferroelectric hysteresis loop.

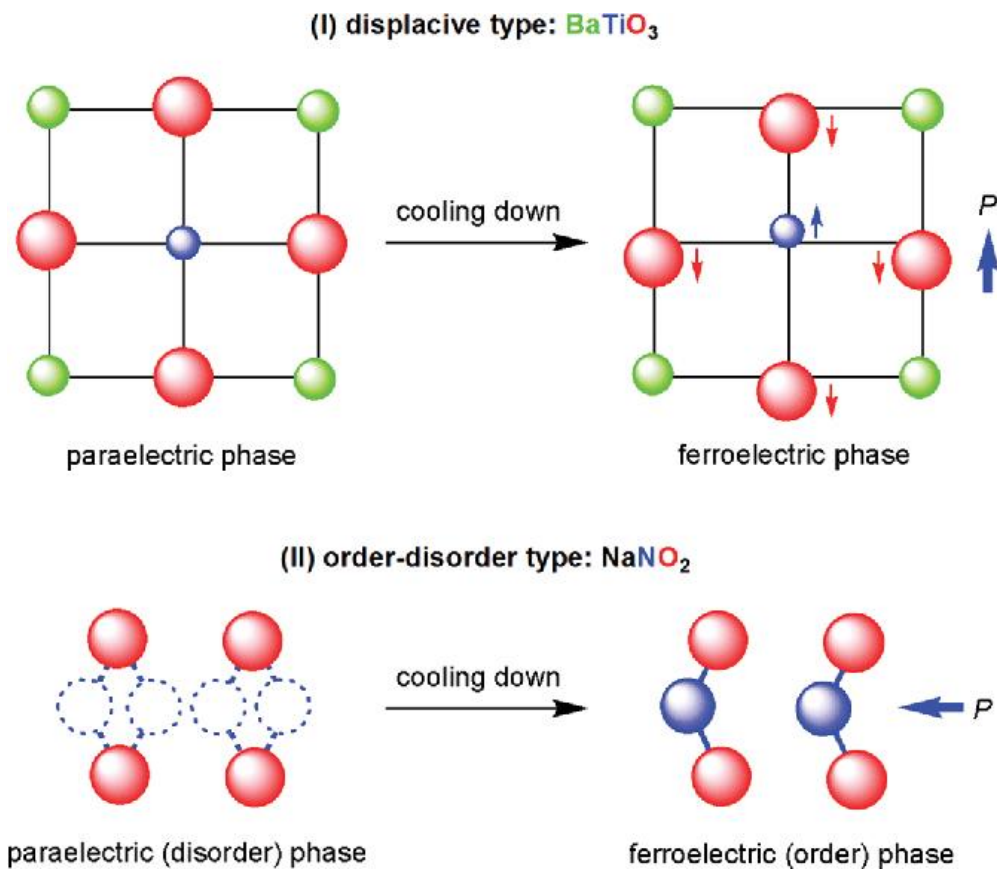


Figure 1.4: Paraelectric-ferroelectric phase transition.

## 1.7 History of Ferroelectric Materials

In 1920, Valasek first discovered the ferroelectric behaviour in the crystal of Rochelle salt.<sup>15</sup>  $\text{KH}_2\text{PO}_4$  (KDP) was the first hydrogen-bonded ferroelectric introduced by Busch and Scherrer.<sup>17</sup> Later barium titanate ( $\text{BaTiO}_3$ ; BTO), first non-hydrogen bonded ferroelectric was discovered in early 1940s. Most commercially used ferroelectrics are inorganic ceramics with perovskite structure such as lead zirconatetitanate (PZT),  $\text{LiNbO}_3$ , and barium titanate (BTO), etc., they displayed excellent polarization responses, the higher value of  $T_c$  and dielectric constant but they exhibit some limitations because of the requirement of high cost, complex synthesis, high-temperature processing and most importantly it contains the potential toxic element lead. This prompted the researchers to look for alternative ferroelectric materials. Recently, ferroelectric materials based on organic, metal-organic, charge-transfer, liquid crystalline systems gained considerably importance because of the flexibility, easy synthesis, absence of toxic elements and low temperature processing.<sup>9,19,20</sup>

## 1.8 Application of Ferroelectric Materials

Based on their switchable spontaneous electric polarization, these materials are mainly used in memory devices and field-effect transistors. Ferroelectric materials also show piezoelectricity, pyroelectricity and high dielectric constant which leads their utility in transducers, micro-electro-mechanical systems (MEMS), actuators, microsensors, etc. Due to their attractive properties they are also used in electro-optical devices, light deflectors etc.<sup>21-24</sup>

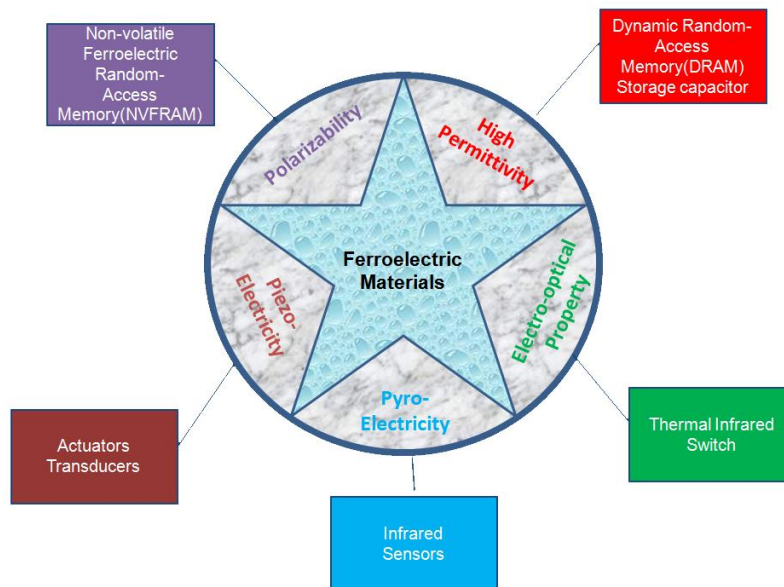


**Figure 1.5:** Applications of ferroelectrics.

## 1.9 Metal-Organic Ferroelectric Materials

Metal-organic ferroelectric materials consists of organic and inorganic parts (ligands, linkers, solvent, metal ions etc.) and hence also referred to as metal organic-inorganic hybrid assemblies. Organic components give various advantages like the variation in structure, tenability and flexibility. In these assemblies, ligands interact with metal ions via many interactions such as hydrogen bonding, ionic, coordination interaction etc.).<sup>25</sup> Rochelle salt is the first metal-organic ferroelectric material.<sup>15</sup>By using building blocks with three-fold symmetry and chiral linkers without coordinating polar head non-centrosymmetric arrangement in metal-organic frameworks can be achieved. The mechanism behind these systems showing ferroelectricity involves the ordering of disordered counter anions, encapsulated guest solvent molecules, distortions around the metal centre and rotation of ligand which bridges metal ions.<sup>26,27</sup>

There are several ferroelectric metal-organic frameworks, which crystallize in polar point group but observed ferroelectric polarization values, and transition temperatures are far from the practical utility, except for few. To date, various interesting families of metal organic assemblies derived from phosphorous based ligands have been reported. These materials exhibit different properties such as ferroelectric, dielectric, solvent sorption properties, host guest chemistries, thermochromic and mechanochromic behaviour etc.

Thus this thesis aims:

- to synthesize and characterize new polar metal organic cages by using a phosphorous based flexible ligand.
- to study the ferroelectric , dielectric and solvent dependent behaviour of metal-organic cages.

# Chapter 2

## Materials and Methods

### 2.1 General Remarks

The phosphoryl chloride was purchased from Sigma-Aldrich and used after distillation because it is very sensitive to moisture. All other chemicals used in synthesis were purchased from Sigma-Aldrich and used without any further purification. NMR spectra were recorded on Bruker Advanced 400 MHz DPX spectrometer at room temperature using 1,1,1,1-tetramethyl silane (TMS) as an internal standard. Data of thermogravimetric analysis (TGA) was obtained from Perkin-Elmer STA 1000 thermogravimetric analyzer. The powder X-ray diffraction (PXRD) data was measured on Bruker-D8 Advance diffractometer. Spectra for FT-IR were obtained in ATR mode on neat samples on a Bruker Alpha spectrophotometer.

### 2.2 Synthesis

#### 2.2.1 Synthesis of ligand [PO(NH<sup>3</sup>Py)<sub>3</sub>] (TPPA):

In the well stirred solution of 3-aminopyridine (7g, 0.075mol) in toluene (~100 ml) the solution of POCl<sub>3</sub> (1ml, 0.01mol) in toluene (20 ml) was added dropwise (POCl<sub>3</sub>&3-aminopyridine was taken in 1:7 ratio). Then solution mixture was refluxed for 12 hrs.<sup>25</sup> Formation of TPPA was confirmed by NMR and MALDI-TOF. We got a yield of 70.55%.

#### 2.2.2 Synthesis of compound [Cu<sub>6</sub>(H<sub>2</sub>O)<sub>12</sub>(TPPA)<sub>8</sub>].(NO<sub>3</sub>)<sub>12</sub>.(H<sub>2</sub>O)<sub>24</sub>

The solution of Cu(NO<sub>3</sub>)<sub>2</sub>.6H<sub>2</sub>O (27.76mg,0.1149mmol) in water (1ml) was carefully dropwise added to a well stirred solution of TPPA ligand (50mg, 0.1532mmol) in MeOH (3ml). The resultant mixture was filtered by celite filtration and kept in 10ml vial, at room temperature in an undisturbed way. After 2-3 weeks, we got blue coloured crystals of compound 1 which were suitable for single-crystal X-ray diffraction analysis.

### 2.3 Crystallography

The diffraction data were collected on a Bruker Smart Apex Duo diffractometer using Mo K $\alpha$  radiation ( $\lambda = 0.71073 \text{ \AA}$ ). The structure was refined by full-matrix least-squares on F<sup>2</sup> using SHELXL program. Crystallographic data for compound 1 are listed in Table 2.1

**Table 2.1:**Details of crystallographic data collection

<b>Compound</b>	<b>1</b>
<b>Chemical formula</b>	C <sub>120</sub> H <sub>192</sub> Cu <sub>6</sub> N <sub>60</sub> O <sub>80</sub> P <sub>8</sub>
<b>Formula weight</b>	4380.44
<b>Temperature</b>	100(2) K
<b>Crystal system</b>	Tetragonal
<b>Space group</b>	I4
<b>a (Å); α(°)</b>	21.14Å; 90
<b>b (Å); β(°)</b>	21.14 Å; 90
<b>c (Å); γ (°)</b>	23.96 Å;90
<b>V (Å<sup>3</sup>); Z</b>	10710(4); 2
<b>ρ (calc.) mg m<sup>-3</sup></b>	2.132
<b>2θ<sub>max</sub> (°)</b>	50
<b>R(int)</b>	0.1237
<b>Data / param. GOF</b>	1.938
<b>R1 [F&gt;4σ(F)]</b>	01150
<b>wR2 (all data)</b>	0.3177
<b>max.peak/hole (e.Å<sup>-3</sup>)</b>	1.401/-1.058

## 2.4 Ferroelectric and Dielectric measurements

To determine the ferroelectric and dielectric properties, powder sample of compound 1 was compacted into pallets of 6 mm diameter and 1 mm thickness. Later, aluminium adhesive foils were attached to pallets which eventually act as electrodes for both measurements. The frequency-dependent dielectric measurements were carried out on the Novocontrol dielectric spectrometer at different temperatures. The P-E loop measurements were performed on the powder pressed pallet of compound 1 using Sawyer-Tower circuit at room temperature for different frequencies. During hysteresis loop measurements time-dependent leakage current for various voltage was measured.

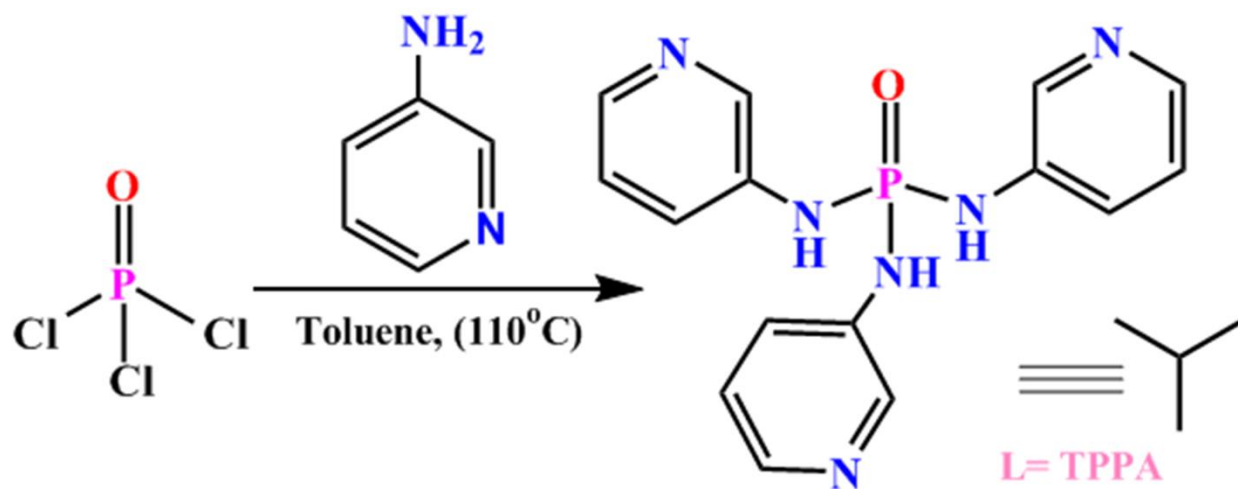
# Chapter 3

## Results and Discussion

### 3.1 Syntheses

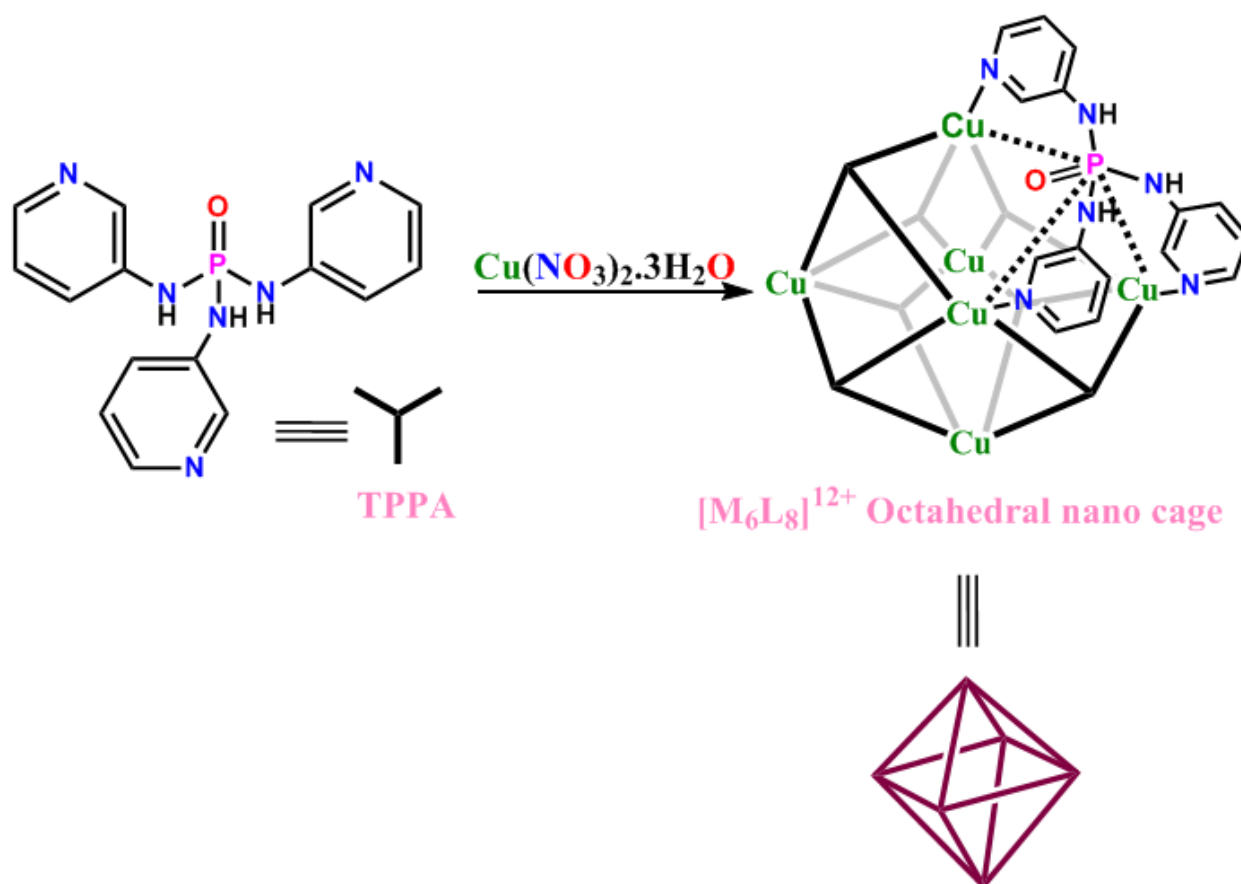
The tripodal ligand TPPA was synthesized from  $\text{POCl}_3$  and 3-aminopyridine in toluene as mentioned by M. Hong and co-workers.<sup>25</sup> It is easily soluble in MeOH. In TPPA ligand the central phosphoryl group and three pyridyl rings are connected by imino groups. Presence of -NH- group reduces rigidity and provides flexible arm to a ligand. It is propeller-shaped tridentate ligand with pyramidal geometry.

#### Scheme 3.1: Synthesis of ligand TPPA



The flexible TPPA ligand adopts various conformation as per the requirement of coordination geometry of metal ions in the assembly process. The reaction of TPPA ligand with  $\text{Cu}(\text{NO}_3)_2 \cdot 6\text{H}_2\text{O}$  in a ratio of 4:3 at room temperature resulted in the formation of the cationic discrete octahedral cage  $[\text{Cu}_6(\text{H}_2\text{O})_{12}(\text{TPPA})_8] \cdot (\text{NO}_3)_{12} \cdot (\text{H}_2\text{O})_{24}$  (compound **1**). The blue coloured crystals of compound **1** are soluble in common polar solvents such as methanol, acetonitrile etc.

### Scheme 3.2: Schematic of Compound 1 formation



### 3.2 Crystal Structures

The X-ray crystallographic analysis reveals that compound **1** form a discrete octahedral cage of  $\text{M}_6\text{L}_8$  type.  $\text{M}_6\text{L}_8$  coordination cage is an important species among discrete metal-ligand assemblies. The crystal structure of compound **1** was solved in the tetragonal space group  $I4$ . The octahedral cage consists of six hexa-coordinated Cu(II) metal ions and eight TPPA ligands. Each Cu(II) ions equatorially coordinated with  $\text{N}_{\text{pyridyl}}$  donor site belonging to four different ligands and axially connected with two water molecules of solvent. We can consider an imaginary octahedron formed by all six Cu(II) metal ions. All eight TPPA ligands present in the discrete cage are in syn conformation with respect to P=O group. There are three 4-fold axes passing through Cu(II) metal ions (Figure 3.1.b) and four 3-fold axes contain P=O groups of TPPA ligands (Figure 3.1.a). The cavity of the cage is filled with water molecules and inward-facing P=O moieties which makes hydrophilic environment inside the cage. Free water molecules and nitrate ions are present disorderly in between the pockets of the cage.

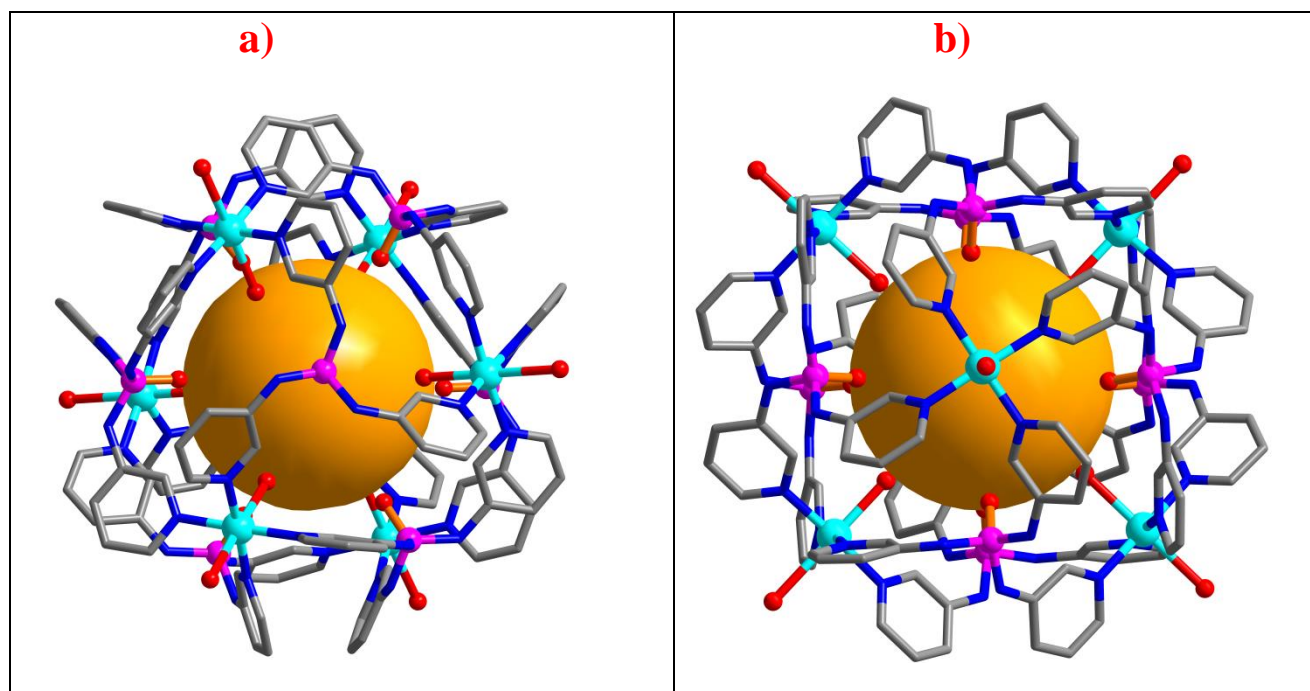


**Figure 3.1:** View of compound **1** octahedral cage along (a) 3- fold and (b) 4-fold axes

### 3.3 Ferroelectric and Dielectric Studies

Compound **1** crystallises in  $I4$  space group and the space group  $I4$  belongs to non-centrosymmetric polar crystal class which motivated us to probe the ferroelectricity in this assembly.

#### 3.3.1 Ferroelectric Results:

Ferroelectric hysteresis loop is the most important observation about ferroelectric materials. The ferroelectric measurement was performed on the powder pressed pallet of compound **1**, it gives a well resolved rectangular loop at a frequency of 0.1 Hz (Figure 3.2). The hysteresis loop indicates the remnant polarization ( $P_r$ ) values of  $39.23 \mu\text{C}/\text{cm}^2$  and saturation polarization ( $P_s$ )  $19.56 \mu\text{C}/\text{cm}^2$ . The value of  $P_s$  is lesser than  $P_r$  indicate that domains formed by the ordering of nitrate ions and solvate ions require high relaxation time. The obtained coercive field ( $E_c$ ) value is 0.64 kV/cm; this noticeably low value of  $E_c$  shows that ferroelectric domains of compound **1** are easily switchable. Leakage current vs. applied field plot reveals low leakage current in the range around  $10^{-6}$  to  $10^{-7} \text{Acm}^{-2}$  and exhibit peaks correlated to the domain switching which is the typical characteristic of ferroelectric materials. The ferroelectric response is due to the ordering of disordered nitrate ions and solvate molecule which is present between the pockets of the cages.

Frequency plays an important role in the polarization of ferroelectric materials. The frequency-dependent studies of P-E loop shows a significant decrease in the  $P_r$  values when increasing the



AC frequency showing the switching rate strongly affects the dynamics of the domain walls (when electric field switching is fast vanishing of domain walls becomes slow and vice versa).

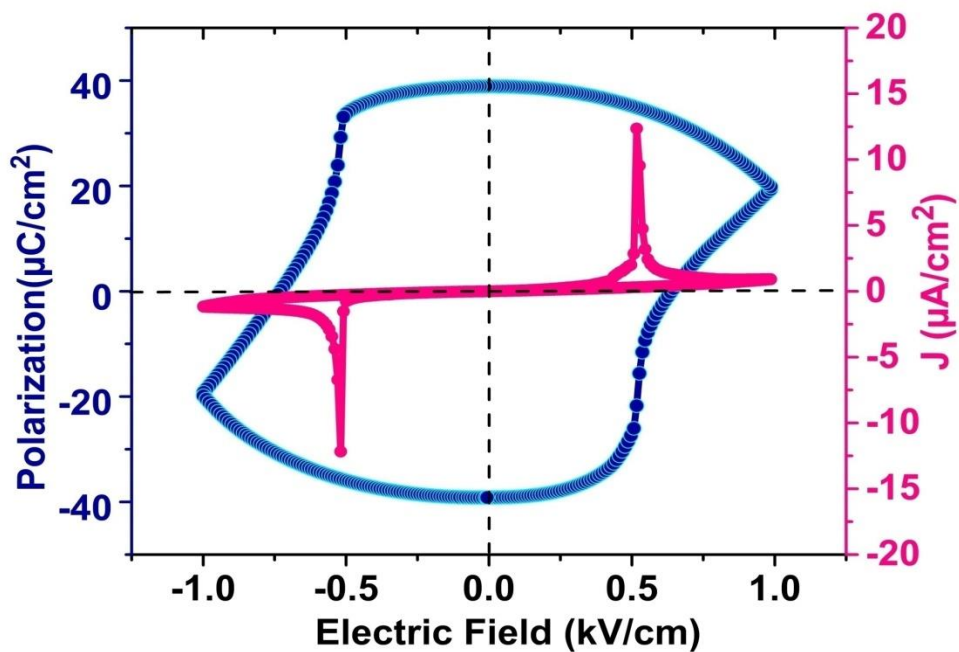


Figure 3.2: Ferroelectric hysteresis loop for compound 1 at frequency 0.01 Hz.

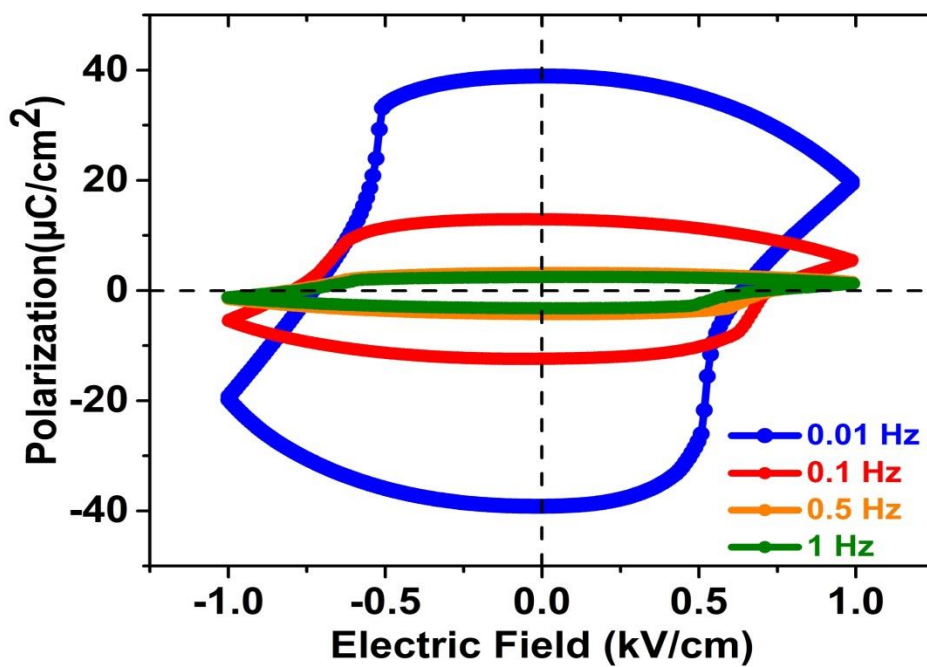
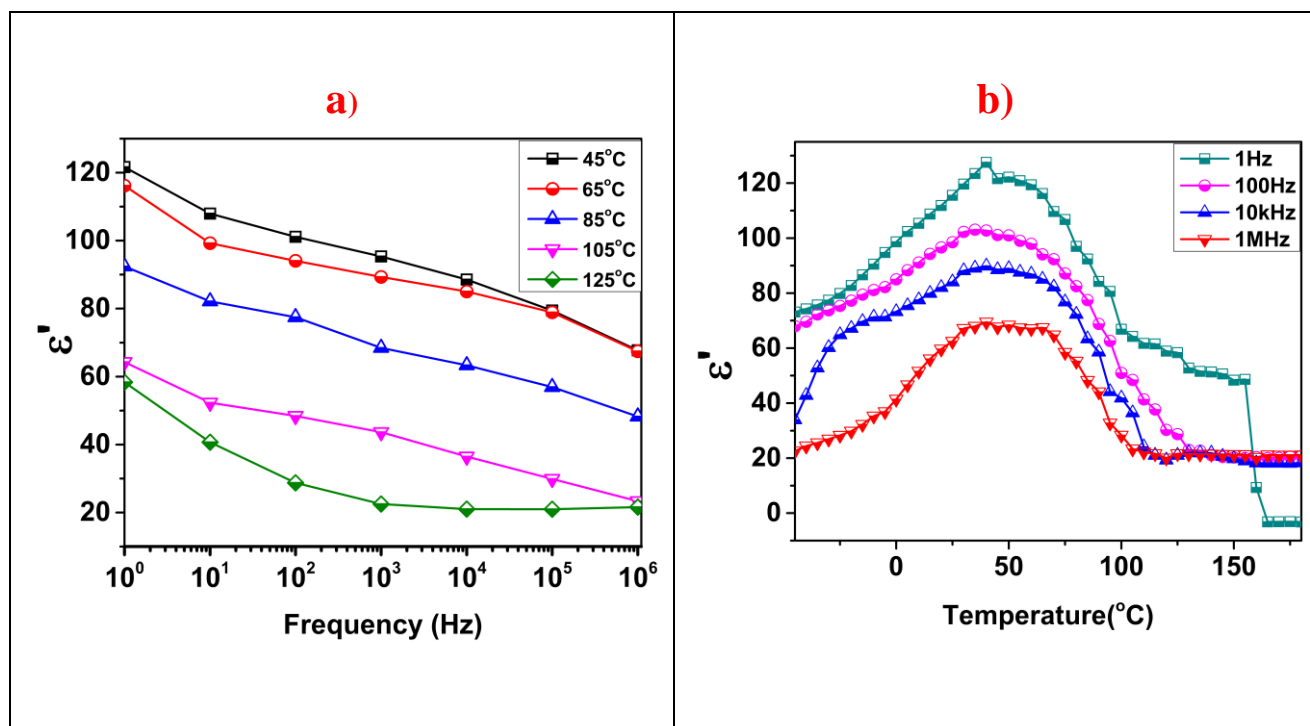


Figure 3.3: Frequency dependent P-E loop studies.

### 3.2.2 Dielectric studies:

Further, dielectric measurements were performed on pallets of compound **1**. The plot of the real part of dielectric permittivity ( $\epsilon'$ ) vs. frequency at different temperatures indicates the maximum  $\epsilon'$  value of 124.4 at a frequency of 1 Hz at 45 °C (Figure 3.4.a). From the nature of the obtained graph it is apparent that decreasing as frequency increases the value of  $\epsilon'$  decreases. This shows that at lower frequencies there are enhanced contributions of all mechanism of polarisation. The graph of  $\epsilon'$  as a function of temperature at different frequencies ranges between 1 to  $10^6$  Hz shows  $\epsilon'$  maxima around 45°C and the highest value is 124.4 at 1 Hz. The intensity of  $\epsilon'$  peak decreases at a higher frequencies. The real part of dielectric permittivity first increases up to 45 °C and then further decreases at a higher temperature (figure 3.4.b). The plot of dielectric loss at different frequencies shows less dielectric loss which confirms the high dielectric nature of compound **1**(figure 3.5.a). At the temperature rises above 100 °C the higher dielectric loss was observed due to desolvation of the compound **1**(figure 3.5.b).



**Figure 3.4:** Plots of the real part of the dielectric permittivity (a) vs. frequency, (b) vs. temperature.

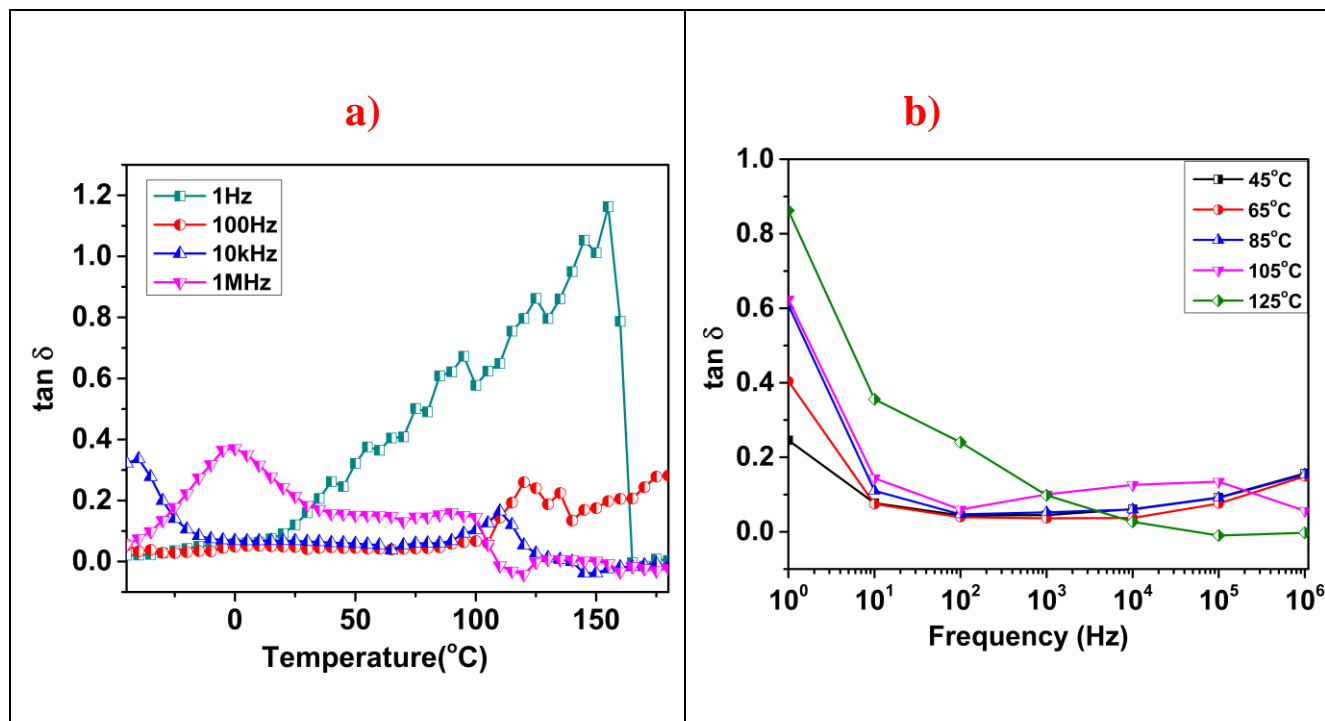


**Figure 3.5:** Plots of the dielectric loss (a) as a function of temperature, (d) as a function of frequency.

## 3.4 Solvent dependent studies of Compound 1

### 3.4.1 TGA

Thermogravimetric differential analysis of compound **1** shows weight loss around 100  $^{\circ}\text{C}$  which correspond to the loss of water molecule . There is a sudden drop of heat flow around 225  $^{\circ}\text{C}$  in the heat flow vs. temperature plot which corresponds to the melting point of compound **1** (Figure 3.6.a). TGA studies of **1**<sub>desolvated</sub> compound (removal of solvent molecules) shows no weight loss related to water molecules and for **1**<sub>resolvated</sub> compound (addition of mother liquor to desolvated compound) there is weight loss corresponding to water molecules (figure 3.6.b).

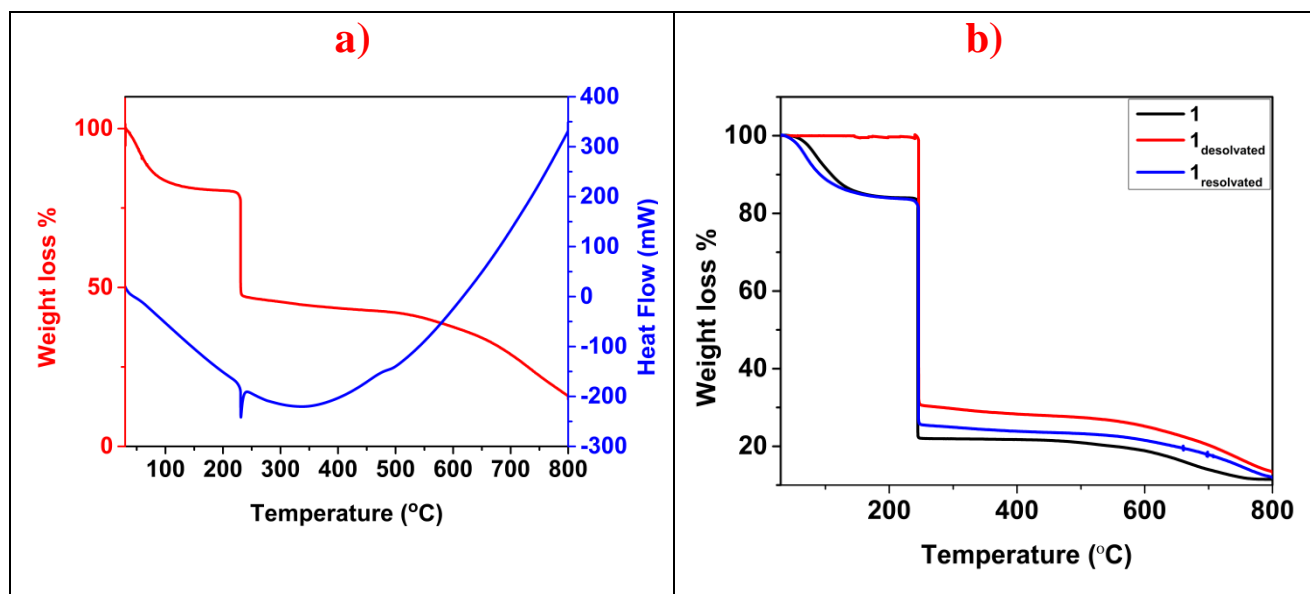


Figure 3.6: a) TGA & DTA plots of as-synthesized (**1**), b) TGA plots of **1**, **1<sub>desolvated</sub>**, and **1<sub>resolvated</sub>**

### 3.4.2 FT-IR

Fourier-transform infrared spectra were measured for all three samples **1**, **1<sub>desolvated</sub>** and **1<sub>resolvated</sub>**. FT-IR spectra of all show similar peak patterns excluding peak related to -OH stretching frequencies of solvated molecules. In the case of **1<sub>desolvated</sub>** it is absent as expected. Whereas, both **1** and **1<sub>resolvated</sub>** have peak for -OH stretching of solvent species (figure 3.7).

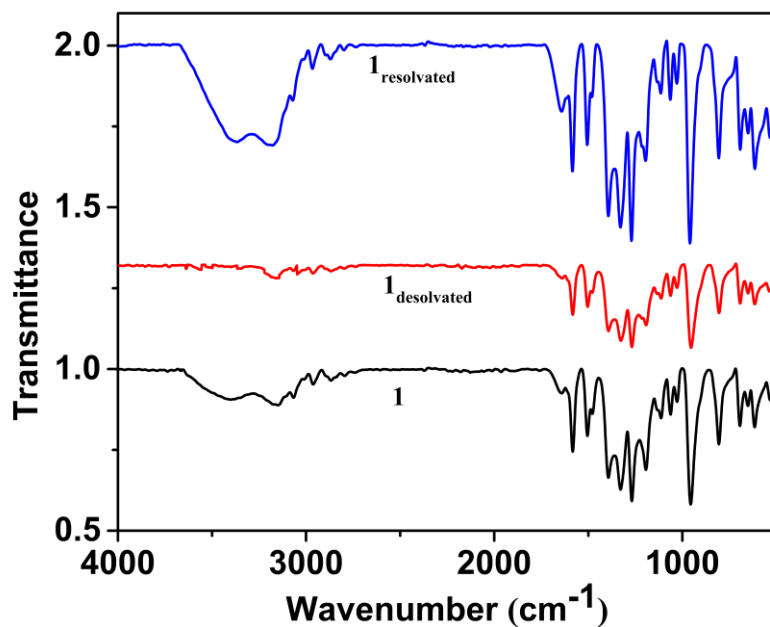


Figure 3.7: IR spectra for **1**, **1<sub>desolvated</sub>**, and **1<sub>resolvated</sub>**.

### 3.4.3 PXRD

Powder X-ray diffraction analysis confirms the formation of compound **1** as all peak patterns of simulated peaks from the single crystal X-ray structure matches with those of the as-synthesized compound **1**. Further, desolvated compound the PXRD pattern does not match with as-synthesized, whereas peak patterns of the resolvated compound exactly resembles with that of the as-synthesized which confirms the reversible nature of process (figure 3.8).

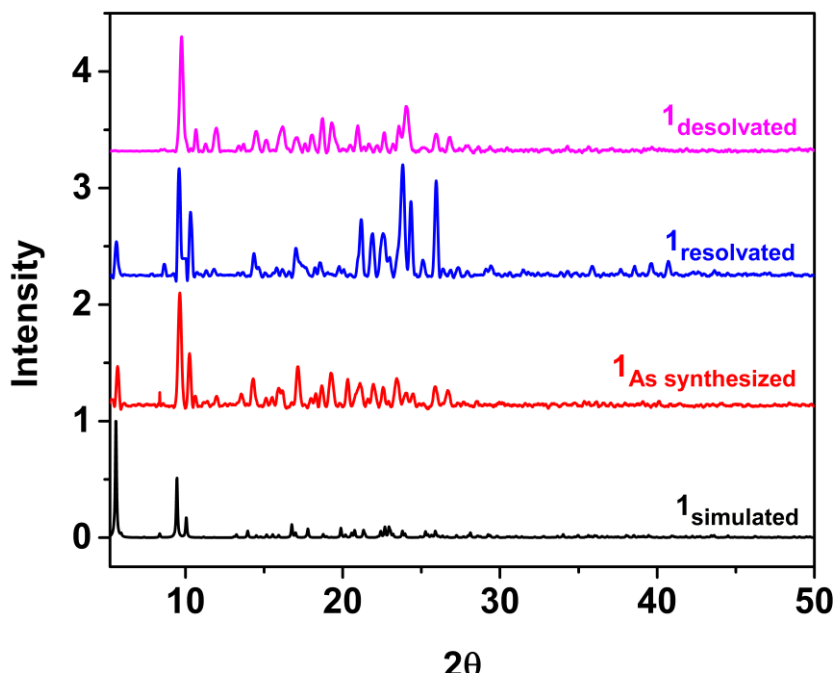


Figure 3.8: PXRD pattern of **1**, **1<sub>desolvated</sub>**, and **1<sub>resolvated</sub>**.

# Conclusion

- We have synthesized a new cationic discrete octahedral cage  $[\text{Cu}_6(\text{H}_2\text{O})_{12}(\text{TPPA})_8](\text{NO}_3)_{12}(\text{H}_2\text{O})_{24}$  with non-centrosymmetric and polar space group *I4*.
- Counterion plays vital role in properties of metal-organic cages as cage formed by the treatment of TPPA with  $\text{Cu}(\text{NO}_3)_2 \cdot 6\text{H}_2\text{O}$  shows well-resolved rectangular P-E loop and the literature reported cage  $[\text{Cu}_6(\text{TPPA})_8(\text{H}_2\text{O})_6](\text{ClO}_4)_{12}(\text{H}_2\text{O})_{24}$  shows no ferroelectricity.
- Compound **1** shows a  $P_r$  value  $39.23 \mu\text{C}/\text{cm}^2$ ,  $P_s$  value of  $19.56 \mu\text{C}/\text{cm}^2$  and  $E_c$  of  $0.64 \text{ kV}/\text{cm}$ .
- The ferroelectric response in compound **1** is due to the ordering of disordered nitrate ions and solvate molecule which is present between the pockets of the cages.
- Frequency-dependent P-E loop studies suggest that the switching rate strongly affects the dynamics of the domain walls.
- Solvent dependent studies confirm the reversible nature of desolvation and resolvation in compound **1**.

# References

1. Whitesides, G. M.; Boncheva M. *Proc. Natl. Acad. Sci. U.S.A.* **2002**, *99*, 4769.
2. Cook, T. R.; Zheng, Y.-R.; Stang, P. *J. Chem. Rev.* **2013**, *113*, 734.
3. Stupp, S. I.; Palmer, L. C. *Chem. Mater.* **2014**, *26*, 507.
4. Long, J. R.; Yaghi, O. M. *Chem. Soc. Rev.* **2009**, *38*, 1213.
5. Richardson, D. W. *Modern ceramic engineering: properties, processing, and use in design*. CRC press: 2005.
6. C.P.Smyth, Annual Review of Physical Chemistry. **1966**, *17*, 433.
7. Rosenberg, H. M. *The Solid State* oxford university press 1988
8. “<http://nptel.ac.in/courses/113104005/68>”, Electro Ceramics Web Course (NPTEL), by Prof.AshishGarg.
9. Zhang, W.; Xiong, R.-G. *Chem. Rev.* **2012**, *112*, 1163.
10. Kasap, S. O. *Principles of electronic materials and devices* Vol. 784. McGraw-Hill New York: 2006.
11. Keppens, V. *Nat. Mater.* **2013**, *12*, 952.
12. C.P.Smyth, Annual Review of Physical Chemistry. **1966**, *17*, 433.
13. W.H.Rodebugh and C.R.Eddy *J. Chem. Phys.* **1940**, *8*, 424.
14. Frohlich, H. *The theory of dielectrics*, London, Oxford university press, Second edition.
15. Valasek, J. *Phys. Rev.* **1921**, *17*, 475-481.
16. Fu, D. W.; Cai, H. L.; Liu, Y. M.; Ye, Q.; Zhang, W.; Zhang, Y.; Chen, X. Y.; Giovannetti, G.; Capone, M.; Li, J. Y.; Xiong, R. G. *Science* **2013**, *339*, 425.
17. Busch, G.; Scherrer, P. *Naturwissenschaften* **1935**, *23*, 737.
18. Cross, L. E. *Ferroelectric Ceramics: Tailoring Properties for Specific Applications*. In: *Ferroelectric Ceramics. Monte Verità* (Proceedings of the Centro Stefano Franscini, Ascona). Birkhäuser Basel: 1993.
19. Horiuchi, S.; Tokura, Y. *Nat. Mater.* **2008**, *7*, 357.
20. Tayi, A. S.; Kaeser, A.; Matsumoto, M.; Aida, T.; Stupp, S. I. *Nat. Chem.* **2015**, *7*, 281.
21. Das, S.; Appenzeller, J. *Nano Lett.* **2011**, *11*, 4003.
22. De Araujo, C. A-P.; Cuchiaro, J. D.; McMillan, L. D.; Scott, M. C.; Scott, J. F. *Nature* **1995**, *374*, 627.
23. Han, S.-T.; Zhou, Y.; Roy, V. A. L. *Adv. Mater.* **2013**, *25*, 5425.
24. Scott, J. F.; De Araujo, C. A. P. *Science* **1989**, *246*, 1400.
25. Li, X.; Jiang, F.; Wu, M.; Zhang, S.; Zhou, Y.; Hong, M. *Inorg. Chem.* **2012**, *51*, 4116-4122.
26. Yadav, A.; Kulkarni, P.; Praveenkumar, B.; Steiner, A. *Chem. Eur. J.* **2018**, *24*, 14639–14643.
27. M. Guo, H.-L. Cai, R.-G. Xiong, *Inorg. Chem. Commun.* **2010**, *13*, 1590–1598.
28. Li, N.; Jiang, F.; Chen, L.; Li, X.; Hong, M. *Chem. Commun.*, **2011**, *47*, 2327–2329.

29. Yadav, A.; Srivastava, A. K.; Kulkarni, P.; Divya, P.; Steiner, A.; Praveenkumar, B.; Boomishankar, R. *J. Mater. Chem. C* **2017**, *6*, 10624–10629.